1st International Conference on Sensing Technology
November 21-23, 2005 Palmerston North, New Zealand

Signal Processing Methods Implemented in a Novel FBG Sensing System for Vibration/Dynamic Strain Measurement

Xingyuan Xu, Enbang Li, Jiangtao Xi and Joe Chicharo
School of Electrical, Computer and Telecommunications Engineering
Faculty of Informatics, University of Wollongong
Wollongong, NSW 2522, Australia
xx89@uow.edu.au

Abstract

We have demonstrated a novel Fiber Bragg Grating sensing system based on a Fabry-Perot tunable filter for measuring dynamic processes. This system is very suitable for multipoint vibration or dynamic strain detection. However, in some conditions, the response time of Fabry-Perot tunable filter will influence the sensitivity of the sensor that the sensitivity is not kept constant. Therefore, post-processing for the measured vibration signal is necessary to solve this problem. In this paper, the demodulation technique of this system is briefly described and two signal processing methods are introduced to deal with the measured signal to obtain stable measurement of the vibration/dynamic strain over the response time of Fabry-Perot tunable filter. In the experiment, program controlled multipoint dynamic strain detection is successfully implemented by this system with these signal processing methods.

Keywords: Fiber Bragg grating, Fabry-Perot tunable filter, vibration, signal processing

1 Introduction

Vibration measurement is critical to monitor the performance and lifetime of mechanical systems. If a monitor system records the vibration history and warning can be made in time, serious damage and breakdown of the mechanical system can be prevented [1, 2]. The conventional piezoelectric or capacitive based sensors suffer from malfunction due to the presence of high magnetic field and high voltage. They are also limited in practice due to their poor electrical isolation ability [3]. The fiber Bragg grating (FBG) was introduced in 1978. This kind of sensor has following particular merits: inherent electrical isolation property, easy to interrogate and multiplex, wide dynamic range, strong anti-jamming ability and easy to build sensing network [4]. Therefore, amongst these advantages, FBGs become ideal candidates for vibration sensors in sensing field.

There are various FBG vibration sensing systems that have been explored [5-10]. In particular, those based on interferometric encoding via optical phase modulation offered high sensitivity. The FBG vibration sensing system based on Mach-Zehnder, Michelson, Sagnac, and Fabry-Perot (FP) interferometers have been reported in the literature [11-14]. However, few practical systems based on interferometric demodulation techniques have been demonstrated for multiplexed sensor systems due to their relative complexity. As for the sensing system based on the tunable filter, it is easy to implement distributed sensing [15]. However, the key problem for this kind of sensing system is how to interrogate small Bragg wavelength shift signal in the high frequency vibration environment.

We have demonstrated a novel demodulation system based on wavelength-multiplexed FBG sensors and the FP tunable filter for measurement of dynamic strain. In such system, a series predetermined reference driving voltages are sent to the FP tunable filter at an interval of few seconds. In that case, passband central wavelength λ_S of FP tunable filter is fixed during the measurement process for each sensor. The FBG wavelength changes can be tracked by measuring the perturbation of the intensity of the reflected light. By using this method, the FP filter needs not be tuned after choosing the reference driving voltage. Therefore, it will release from the restricted scanning frequency. This system is very suitable for multipoint vibration/dynamic strain detection. However, the response time of FP tunable filter will influence the sensitivity of the sensor that the sensitivity is not kept constant. Hence, post-processing for the measured vibration signal is necessary to solve this problem.

In this paper, the demodulation technique of this system is briefly described and two signal processing methods are introduced to deal with the measured signal to obtain stable measurement of the vibration/dynamic strain over the response time of Fabry-Perot tunable filter. Experiment system is implemented and results are presented.

2 Principle and Methodology

Typically, the Bragg Wavelength shift with strain and temperature can be expressed by using [4].

$$\frac{\Delta\lambda_B}{\lambda_B} = \left(1 - \frac{n^2}{2}\left[\rho_{12} - \nu(\rho_{11} - \rho_{12})\right]\right)\Delta\varepsilon + (\alpha + \xi)\Delta T \quad (1)$$

Where:

$\Delta\varepsilon$ = applied strain
$P_{i,j}$ = Pockel's coef. of the stress-optic tensor
ν= Poisson's ratio
α= coef. of thermal expansion
ξ= thermo-optic coefficient
ΔT = temperature change

The shift in Bragg Wavelength is approximately linear respect to the perturbation of strain and temperature [4]. Therefore, strain-induced FBG wavelength shift can be expressed as:

$$\frac{\Delta\lambda_B}{\lambda_B} = (1 - P_e)\Delta\varepsilon \quad (2)$$

Where P_e is the effective photoelastic constant of the fiber. Therefore, from (2) the strain perturbation can be determined by measuring the corresponding FBG wavelength change.

One of the most successful and attractive demodulation approaches to determine FBG wavelength changes of FBG sensing system is to use a scanning FP tunable filter. The FP tunable filter is driven by the triangular voltage waveform. While the filter is tuned, a piezoelectric actuator changes the cavity length so that the central wavelength of the filter moves, as shown in figure 1. The photocurrent of FP filter is a convolution of both the spectrum of the tunable filter and that of the FBG. When the spectrum of the tunable filter matches that of the FBG, the maximum convolution output occurs. Normally, the photocurrent signal from tunable FP filter is converted into electrical signal by a photo detector. Hence, the output voltages from the photo detector may be expressed using the following integral:

$$V_i(\lambda_S) = \int_{-\infty}^{\infty} \alpha S_{FP}(\lambda, \lambda_S) S_{FBGi}(\lambda, \lambda_{\mathrm{Bi}}) d\lambda \quad (3)$$

Where, $S_{FP}(\lambda, \lambda_S)$ and $S_{FBGi}(\lambda, \lambda_{\mathrm{Bi}})$ are the spectral shapes of the FP filters and FBGs, λ_S is the central wavelength of FP tunable filter, λ_B is the FBG wavelength, α is the constant which presents the receiver optical to electric conversion factor.

The normal method to track the FBG wavelength shift based on the FP tunable filter is to measure the full output voltage values from the photo detector and find the peak value. The FP filter is tuned at a given frequency, by measuring the maximum output voltage value and the corresponding driving voltage for every scanning process, the wavelength shift of the FBG can be obtained. However, the current scanning rate of FP filter is hard to exceed 1 KHz [4], which means it is difficult to track the high frequency FBG wavelength perturbation.

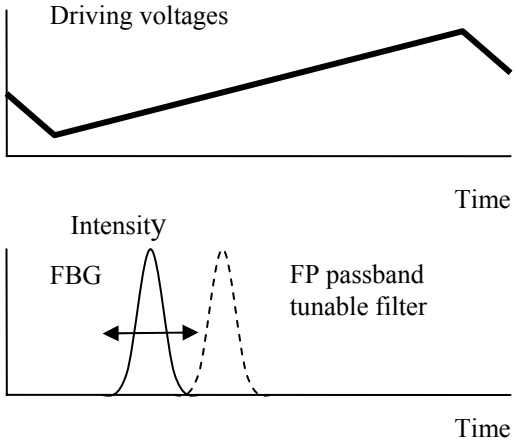

Figure 1 Working principle of FP tunable filter for processing FBG return signal

An alternative method to solve this problem is to set the FP tunable filter at a predetermined reference driving voltage V_R on which the passband central wavelength λ_S is fixed during the measurement process. Using (3), the FBG wavelength changes can be tracked by measuring the perturbation of output voltage V. Supposing that the applied driving voltages for FP tunable filter has linear relationship with the output voltages in a small range, the slope of the reference point can be regarded as the proportion constant between driving voltage and output voltage:

$$V_{out} = V_{driving} \quad a \quad (4)$$

As shown in figure 2, the midpoint of the waveform's rising edge/falling edge has maximum slope value that the output voltage has the highest sensitivity with the driving voltage in this point. Therefore, the driving voltage of this point is regarded as the referencing driving voltage. Besides, the driving voltage is proportional to the FBG wavelength and the ratio coefficient may be identified by calibration test.

$$V_{driving} = F_{FBG}(\lambda_B) \quad (5)$$

Hence, by (2), (4) and (5), the dynamic strain can be determined through measuring the output voltages of FP tunable Filter. By using this method, the FP tunable filter needs not to be tuned after choosing the reference driving voltage. Therefore, it releases from the restricted scanning frequency.

However, because of the response time of FP tunable filter, the driving voltage cannot be sent to the reference point immediately. Setting the reference driving voltage is a dynamic process (from V_I to V_R gradually) as shown in figure 2. Therefore, the DC

offset will be observed in the measured output voltages signal (from $V_{dc\text{-}I}$ to $V_{dc\text{-}R}$). If a series of amplitude fixed dynamic strain is applied to the FBG sensor, the output voltages signal from the FP tunable filter will be an integration of a high frequency signal and a low frequency signal. Figure 3 shows a piece of output voltages signal getting from the demodulation system. The high frequency signal stands for the dynamic strain induced FBG wavelength shift and the low frequency signal represents response characteristic of the FP tunable filter. In this case, the central wavelength of FP tunable filter cannot keep stable during the measurement process. If the slope value of reference point is regarded as the only proportion constant between driving voltage and output voltage, measurement error will occur.

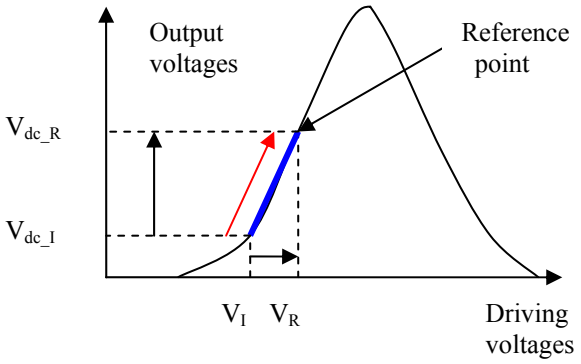

Figure 2 The process of setting the FP tunable filter to the reference point

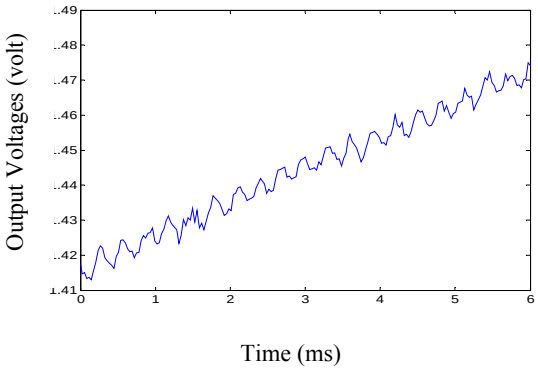

Figure 3 Output of the FP tunable filter include high frequency vibration and low frequency DC offset

Therefore, post-processing for the measured vibration signal is necessary. One method is to separate high frequency and low frequency signal for each measured output voltages signal. Both a 150 order FIR high pass filter and pass filter are used to separate these two signals for each FBG sensor, the separated DC and AC signal is shown in Figure 4 (a) and (b).

From Figure 4(b), it is shown that the amplitude of the AC signal of the output voltage changes along the time axis. The reason is that the relationship between the driving voltages and the output voltages from the FP filter is shifted continuously during that time. Therefore, the slope of the reference point cannot be regarded as the only constant coefficient between the output voltage and driving voltage. To solve this problem, S_{AC} is divided into a number of small pieces and a slope series will be used to represent the relationship between the driving voltages and the output voltages.

$$S_{AC} = \sum_{i=i}^{n} S_i \qquad (6)$$

For each piece of signal S_i, it has almost the same $V_{out} - V_{driving}$ relationship or slope value at each signal point. Therefore, by using different slope values in different pieces of signal, the output voltages can be transformed into the corresponding driving voltages that have invariable amplitude. The vibration frequency and amplitude of driving voltages signal can be obtained by frequency domain analyse. The frequency of scanning voltages signal is same as the frequency of the dynamic strain. And the amplitude of dynamic strain will be calculated utilizing the known relationship by (2), (4) and (5).

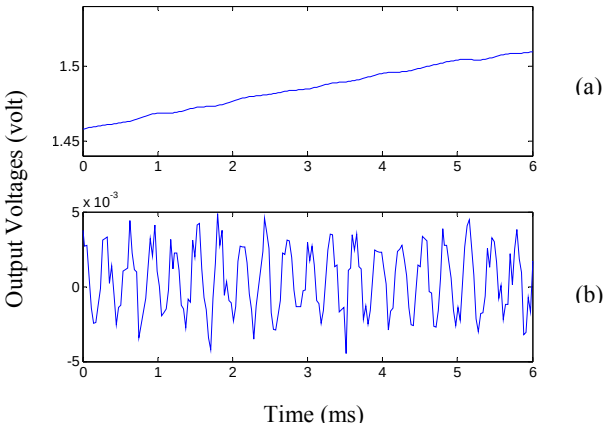

Figure 4 Filtered output signal. (a) DC component and (b) AC component

The other processing method is to fit the relationship between the driving voltage and the output voltage as a formula instead of slope calculation. According to the Gaussian distributions, the expressions for the output voltage from the FP tunable filter can be expressed as:

$$V_{output}(V_{driving}, V_{peak}) = A + V_0 * \exp(-4\ln 2/\alpha^2 (V_{driving} - V_{peak})^2) \qquad (7)$$

Where, A is the offset for the dark noise from receivers, α is the FWHM of the scanned output voltage shape, V_0 is the peak value of the output voltages, $V_{driving}$ is the driving voltages and V_{peak} presents the driving voltage corresponding to V_0.

Then the driving voltages signal can be achieved from the output voltage signal utilizing (5). It still is an integration of a high frequency signal and a low frequency signal. However, the amplitude of the AC

signal will not change along the time axis because the slope changes have been compensated by the formula. It only needs to separate the high frequency signal from the low frequency signal. Using this method, the large amplitude output voltage vibration may be measured more accurately than the slope method.

3 System Description

The system is shown in figure 5. Broadband light is transmitted to the sensor FBGs via a three-port circulator. FBG sensors reflect the light of the relevant Bragg wavelength to the circulator along the transmission optical fiber and reach the tunable F-P filter. The tunable FP filter connects to the photo detector that is used to transfer the photocurrent signal into electrical signal. Then the data acquisition unit gathers the electrical signal. The desktop computer controls both the tunable filter and the data collection unit by Labview program.

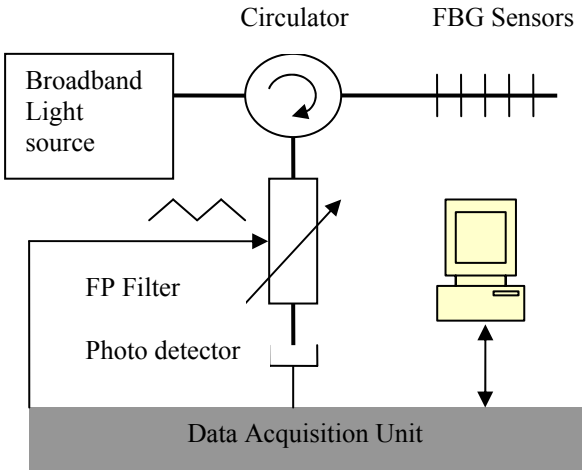

Figure 5: Schematic diagram of FBG vibration detection system

At the beginning of measurement, the desktop computer generates a series of driving voltages to drive the tunable filter to conduct a continuous scanning within its free spectral range (FSR). Then the relationship between the driving voltages and the output voltages is built as a series of individual waveforms. The data acquisition unit records these waveforms and the desktop computer calculates the corresponding driving voltage for the FP tunable filter at the midpoint of each waveform's raising edge/falling edge. Then the desktop computer adjusts the driving voltage of FP tunable filter to the referencing point of the first FBG sensor, and keeps it on this point for a period of time during which the data acquisition unit records the output voltage signal from the photo detector.

After the data collection, the desktop computer controls the FP tunable filter to the referencing point of the second FBG sensor, and repeats the above data collection and record process. Repeat such a process until the measurement is finished for the dynamic wavelength of all FBG sensors. And then come to the following steps: Start from the first FBG sensor to conduct the repetitious measurement; after 3 times measurement, the tunable filter conducts a continuous scanning within FST again, and re-identifies the referencing point of each FBG sensor.

4 Experiments and Results

In order to test the method, an experiment is set up with two fiber Bragg gating sensors in different wavelength. A vibration generator is connected with these two sensors and the output voltages from the photo detector are recorded at the sampled rate 30 KHz by the data acquisition unit. The desktop computer generates a series of driving voltage (0.1~2 volt with the interval of 0.002 volt) to drive the tunable filter to conduct a continuous scanning within FSR. Then the relationship between the driving voltages and the output voltages is built, as shown in figure 6. We use Labview calculates the reference point and implements vibration detection process for two FBG sensors incessantly. The two curves in figure 7 shows the output voltages from the photo detector for two FBG sensors when the driving voltage is sent to the reference points separately.

Then the first processing method is implemented on the output voltage signal. A high pass filter and a low pass filter are used to separate the AC and DC signals for each sensor and the filtered signal is shown in figure 8a and figure 8b.

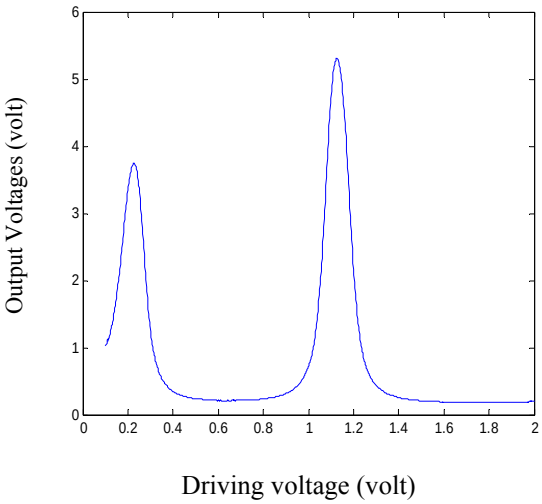

Figure 6 The output voltages of FP tunable filter during the scanning process for two FBG sensors

The vibration signal S_{AC} is divided into a number of small pieces (20 samples each). For each piece of signal, the slope of its mean value needs to be calculated. Utilizing (4), the output voltage signal from the photo detector can be transformed into the driving voltages of FP tunable filter. In order to get the accurate information of the vibration source, it is necessary to analyse the frequency domain

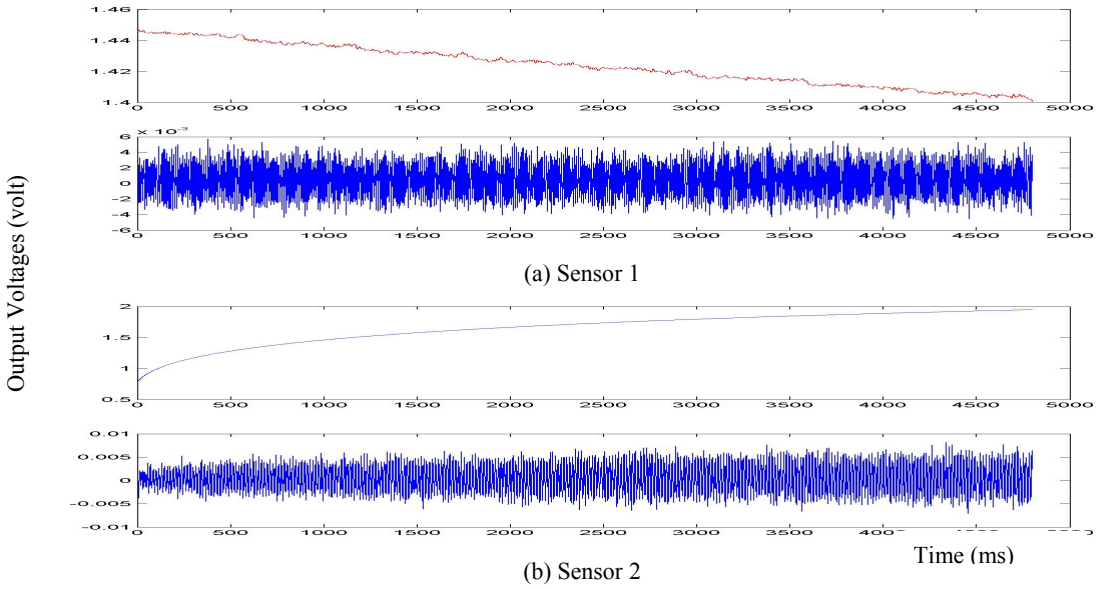

Figure 8 Separated AC and DC signal for 2 sensors

characteristics of the driving voltage signal. It is found that the vibration is combined with one fundamental wave and several noise signals. The frequency of the fundamental wave stands for the frequency of the vibration. The amplitude of the vibration can be acquired by integrating the spectrum of the fundamental wave.

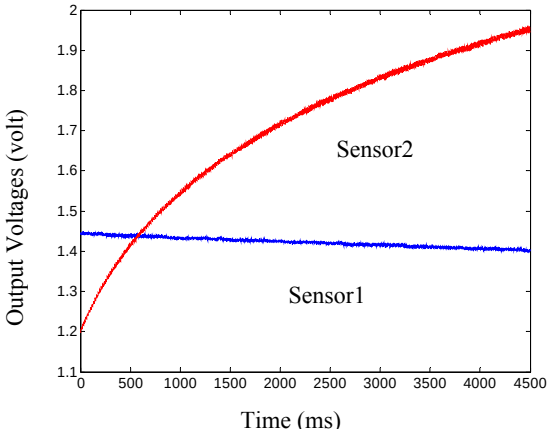

Figure 7 Output voltages of FP tunable filter for two FBG sensors

In this case, the vibration frequency measured in each sensor is 3.0 KHz. Without the signal processing method, the vibration amplitude measured in sensor 1 and sensor 2 using the unique slope value are 4.73 mv and 3.98 mv respectively. The relative measurement error is up to 20%. With the first processing method, vibration amplitude of driving voltage signal at sensor 1 is 5.2 mv, at sensor 2 is 5.41 mv. The experiment results are in accordance with the experiment setting that the amplitudes of the driving voltage signal measured at different sensor are very close.

Then the second processing method is implemented. The relationship of output voltages and driving voltage for the two FBGs is fitted as a formula respectively. Using (5) the expression can be express as:

$$V_{output} = 0.3 + 3.826 * \exp(-167 * (V_{driving} - 0.238)^2) \quad (8)$$

And

$$V_{output} = 0.3 + 5.008 * \exp(-170 * (V_{driving} - 1.126)^2) \quad (9)$$

Utilizing these expressions, the driving voltage signal can be obtained directly. A section of driving voltage signal is shown in figure 9. The measured vibration frequency is 3 KHz and the vibration amplitudes are 5.25mv, 5.36mv for the two FBG sensors respectively, which is very similar with the result we got by the first method.

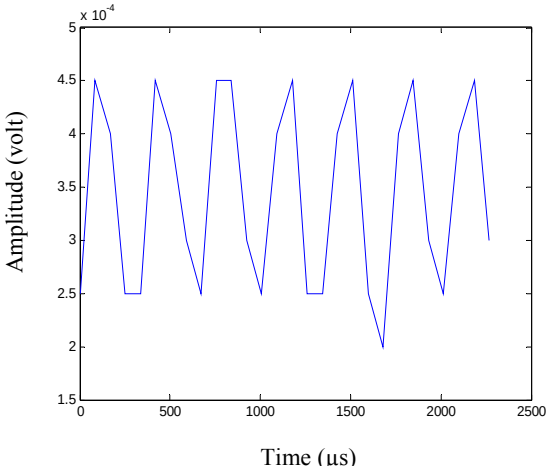

Figure 9 A section of driving voltages signal using curve-fitting method

5 Conclusion

In this paper, two signal processing methods are introduced to deal with the measured signal to obtain stable measurement of the vibration/dynamic strain over the response time of Fabry-Perot tunable filter. During the real-time vibration monitoring, the response time of Fabry-Perot tunable filter will cause the fluctuation of the sensors' sensitivity. And the fluctuation of the sensitivity will produce measurement error. The experimental result shows that the proposed post-processing method can remove such error. Combing these signal processing methods, the FP tunable filter based sensing system is suitable for measuring the high frequency vibration and dynamic strain. This system has some considerable advantages such as high sensitivity, high detect resolution, good multiplexing ability and low cost.

6 References

[1] M. Serridge, "What makes vibration condition monitoring reliable", Noise Vibration Worldwide 22 (8) (1991) 17–24.

[2] J.R. McEwan (Ed.), "Condition Monitoring", vol. 3, Gulf Publishing, Houston, 1991.

[3] M.Lequime, "Fibre sensors for industrial applications", Proceedings of the 12th International Conference on Optical Fibre Sensors, OSA Technical Digest Series, vol. 16, OSA, Washington, DC, 1997, pp. 66–71.

[4] Andreas Othonos, Kyriacos Kalli, "Fiber Bragg grating: fundamental and applications in telecommunications and sensing", Artech House optoelectronics library, 1999.

[5] A. Ezbiri, R.P. Tatam, "Passive signal processing for a miniature Fabry-Perot interferometric sensor with a multimode laser-diode source", Opt. Lett. 20 (17) (1995) 1818–1820.

[6] M. Brenci, A. Mencaglia, A.G. Mignani, "Fiber-optic sensor for simultaneous and independent measurement of vibration and temperature in electric generators", Appl. Opt. 30 (21) (1991) 2947–2951.

[7] L.C.S. Nunes, L.C.G. Valente*, A.M.B. Braga, "Analysis of a demodulation system for Fiber Bragg Grating sensors using two fixed filters", Optics and Lasers in Engineering 42 (2004) 529–542

[8] Ning Y N, Meldrum A, Shi W J,et al. "Bragg Grating Sensing Instrument Using a Tunable Fabry-Perot Filter to Detect Wavelength Variations", Meas.Sci.&Technol, 1998, 9(6):599-606

[9] P.D. Dinev, "A two-dimensional fiberoptic vibration sensor", Meas. Sci. Technol. 6 (1995) 1395–1398.

[10] P.-Y. Chien, Y.-S. Chang, M.-W. Chang, "Vibration suppression in a flexible structure based on fiber optics Michelson interferometric sensor", J. Intelligent Mater. Syst. Struct. 7 (1) (1996) 65–70.

[11] A. Dandridge, A.D. Kersey, "Overview of Mach-Zehnder sensor technology and applications", in: Proceedings of the Fiber Optic Laser Sensors VI SPIE, vol. 985, Boston, 1988, p. 34.

[12] E. Tapanes, "Real-time structural integrity monitoring using a passive quadrature demodulated, localised Michelson optical fibre interferometer capable of simultaneous strain and acoustic emission sensing", Proc. SPIE—Int. Soc. Opt. Eng. 1588 (1991) 356–367.

[13] S.C. Lin, T.G. Giallorenzi, "Sensitivity analysis of the sagnac-effect optical-fiber ring interferometer", Appl. Opt. 18 (1979) 915–931.

[14] V. Bhatia, K.A. Murphy, R.O. Claus, M.E. Jones, J.L. Grace, T.A. Tran, J.A. Greene, "Optical fibre based absolute extrinsic Fabry-Perot interferometric sensing system", Meas. Sci. Technol. 7 (1996) 58–61.

[15] F. Farahi, T.P. Newson, J.D.C. Jones, D.A. Jackson, "Coherence multiplexing of remote fibre optic Fabry-Perot sensing system", Opt. Commun. 65 (5) (1988) 319–321.